ISSN 1063-7842, Technical Physics, 2018, Vol. 63, No. 4, pp. 540–545. © Pleiades Publishing, Ltd., 2018.
Original Russian Text © E.A. Alfyorova, D.V. Lychagin, 2018, published in Zhurnal Tekhnicheskoi Fiziki, 2018, Vol. 88, No. 4, pp. 555–560.

SOLID STATE

Relation between the Hurst Exponent and the Efficiency of Self-organization of a Deformable System

E. A. Alfyorova[a,*] and D. V. Lychagin[a,b,]**

[a] *National Research Tomsk Polytechnic University, Tomsk, 634050 Russia*
[b] *National Research Tomsk State University, Tomsk, 634050 Russia*
**e-mail: katerina525@mail.ru*
***e-mail: dvl-tomsk@mail.ru*

Received July 6, 2017

Abstract—We have established the degree of self-organization of a system under plastic deformation at different scale levels. Using fractal analysis, we have determined the Hurst exponent and correlation lengths in the region of formation of a corrugated (wrinkled) structure in [111] nickel single crystals under compression. This has made it possible to single out two (micro- and meso-) levels of self-organization in the deformable system. A qualitative relation between the values of the Hurst exponent and the stages of the stress–strain curve has been established.

DOI: 10.1134/S1063784218040035

INTRODUCTION

The surface of a crystal reflects the processes of plastic deformation occurring in the bulk. Even at the beginning of the last century, Rosenhein and Eaving, as well as Hirth and Lote [1] showed that the deformation relief consists of lines. These lines are steps on the surface. Such steps appear due to microscopic shears due to the motion of dislocations in slip planes. The traces of shear are observed beginning with small shear strains in single crystals and polycrystals. Their formation is typical of various types of loading. Consequently, these features can be treated as the basic structural element of the deformation relief.

During the evolution of deformation, shear traces in various combinations form elements of the deformation relief of the following scale levels: trace stacks, meso- and macrobands, corrugated structures of various types (wrinkles), persistent slip bands, etc. Corrugated structures (wrinkles) are among the most interesting elements of the deformation relief. Their morphology is very diversified, and they are manifested at different levels [2–16]. Corrugation often accompanies the processing of metals by pressure as an undesirable effect. In publications devoted to this problem, the formation of the texture and the structure of the material after straining are mainly considered [2–5]. It was shown in [6] that corrugation of a metal during rolling is determined by the peculiarities of the flow of different layers of the metal in the deformation center. The formation of a corrugation (protrusions) on the surface of a copper sample deformed by a hard indenter was described in [7]. Analogous results were obtained independently and described in [8]. The formation of corrugated structures and wrinkling under mechanical loading was mentioned in [9, 10]. The formation of corrugation (wrinkling) during deformation of films on substrates was reported in a number of publications [11–15]. It was shown in [15] based on modeling that owing to the formation of corrugation, closely packed planes relax, forming a saddle-shape profile of the surface. In some publications, the formation of corrugated structures on the surface was attributed to excess straining of the surface layer [16] as compared to the inner part of the crystal. In this case, the deformation of the solid is treated as a hierarchic interaction of the elastically deformed layer of the main crystal and the plastically deformed surface layer; i.e., the surface layer is a separate mesoscale layer of deformation [16–18]. This layer possesses a high density of vacancies and dislocations and the lowest shear stability. In [19], three different cases concerning the difference in the degree of hardening of the surface layer and the inner volume of the crystal are indicated: the surface is hardened more strongly than the bulk of the material, the surface is hardened to a lesser degree than the bulk of the material, and the surface layer and the inner volume are hardened identically.

Corrugation (wrinkling) is also typical of single-crystal objects. The authors have made several attempts at classification of the entire variety of corrugated (wrinkled) structures in fcc single crystals [20–23]. It has been established that the [111] orientation is more keen to the formation of corrugations with dif-

ferent morphologies. This is associated with the crystallographic orientation of crystal faces. At the same time, analysis of corrugated structures of single crystals is convenient for establishing physical regularities in connection with certain geometry of dislocation slip and the absence of the grain boundary effects.

Therefore, corrugated structures on the surfaces of deformed crystals can be observed in different cases. The formation of corrugated structures depends on intrinsic properties of a crystal and does not require special external action. A corrugation is formed on the surface of a single crystal from shear traces beginning from a certain strain. Consequently, corrugated structures are structural elements of the deformation relief of a qualitatively different level as compared to shear traces. The facts listed above are essentially the features of a self-organizing system. The aim of such self-organization is obviously the tendency of the crystal to preserve its integrity under loading for as long as possible (increase of the longevity of a loaded system).

In this connection, this study aims at establishing the regularities of self-similarity and, hence, self-organization of a corrugated structure in the course of deformation of single crystals, the determination of the features of the local distribution of stresses in the zone of corrugation formation and its ability to stress relaxation.

1. MATERIAL AND TECHNIQUE

As the object of investigation, we chose a nickel single crystal (with a purity of 99.99%) with the [111] orientation of the contraction axis. Compression strain was carried out on the Instron ElektroPuls E10000 test machine at a rate of 1.4×10^{-3} s^{-1}. The deformation relief was investigated using an Olympus LEXT OLS4100 confocal laser scanning microscope. The size of the scanned region in each case was 0.066 mm^2 (0.256×0.256 mm^2). The depth resolution was 0.06 μm. Experiments were carried out in the strain interval 1.5–18%. The size of the scanned region in this case sets a limit on the self-organization scale being established.

For revealing scale-invariant regularities of plastic straining of nickel single crystals under compression, we used fractal analysis of the deformation relief based on the height–height correlation function $H(r)$ [24, 25]

$$H(r) = \langle [Z(r') - Z(r' - r)]^2 \rangle,$$

where $Z(r)$ is the function of the surface height over all pairs of points separated by a fixed distance r; angle brackets indicate averaging over all pairs of points.

The slope of the initial segment of the curve describing the height–height correlation function $H(r)$ and plotted in logarithmic axes can be used for determining the Hurst exponent (H) and correlation length L. The correlation length is determined by the projection of the linear segment onto the abscissa axis.

2. RESULTS AND DISCUSSION

We have investigated the evolution of the deformation relief on the (112) lateral face of a [111] nickel single crystal. Here, we report on the results obtained for the region of the lateral face, which is occupied by corrugated (wrinkled) structures. The region under investigation is at the center of the face near the vertical edge of the sample. At the initial strains, this zone is in the uniaxial compression region. However, with increasing compression ratio, the scheme of the stressed state passes to a more complex extension–compression case due to the macroscopic change in the sample shape [26]. The corrugation (wrinkled) type formed in this region has a clearly manifested and single smooth boundary. Within the corrugation region, a system of shear traces can be observed. One side of the corrugation is more gently sloping, while the other is steeper relative to the plane of the face. The folds are formed quasi-parallel to one another. Such a type of deformation relief was also observed in our experiments with copper single crystals and was considered in detail in [23].

The deformation relief and the change in the surface profile is illustrated in Fig. 1. The surface profile was determined on the surface in the direction perpendicular to the wrinkles; the Y axis was perpendicular to the surface of the face. Shear traces and wrinkles appear for a total strain of 1.5% of the sample. This is reflected in the profile of the cutting plane in the region of the relief formation on the surface (Fig. 1b). With increasing strain, wrinkled structures on the surface become manifested more clearly (Figs. 1a, 1c–1e). On the surface profile, such structures have the form of alternating regions of material extrusion and intrusion (quasi-periodic profile). On the profile, we can always single out shear steps h (Fig. 1f). With increasing strain, the shape of the surface profile changes. At a strain of 8%, we observe more rounded pits, but with increasing deformation, a tendency to deepening and sharpening of the pits can be traced. The extrusion regions lose their rounded profile and acquire a pointed shape with some roughness at the tips. In addition, the number of extrusion/intrusion zones on a segment under investigation increases.

Analysis of the 3D pattern and the surface profile in the region of formation of corrugated structures suggests a mounded form of the surface. It is well known that there are surfaces characterized by undulated formations with a regular arrangement of "mounds" [27, 28]. Such surfaces have a characteristic long-range scale of length (wavelength) λ, which is a measure of the spacing between the mounds.

The existence of the mounded surface can be judged from the height–height correlation function $H(r)$, power spectrum density (PSD) functions, and autocorrelation function $A(r)$. Quantity λ (wavelength, distance between mounds) can be determined as the value of r that corresponds to the first minimum of the

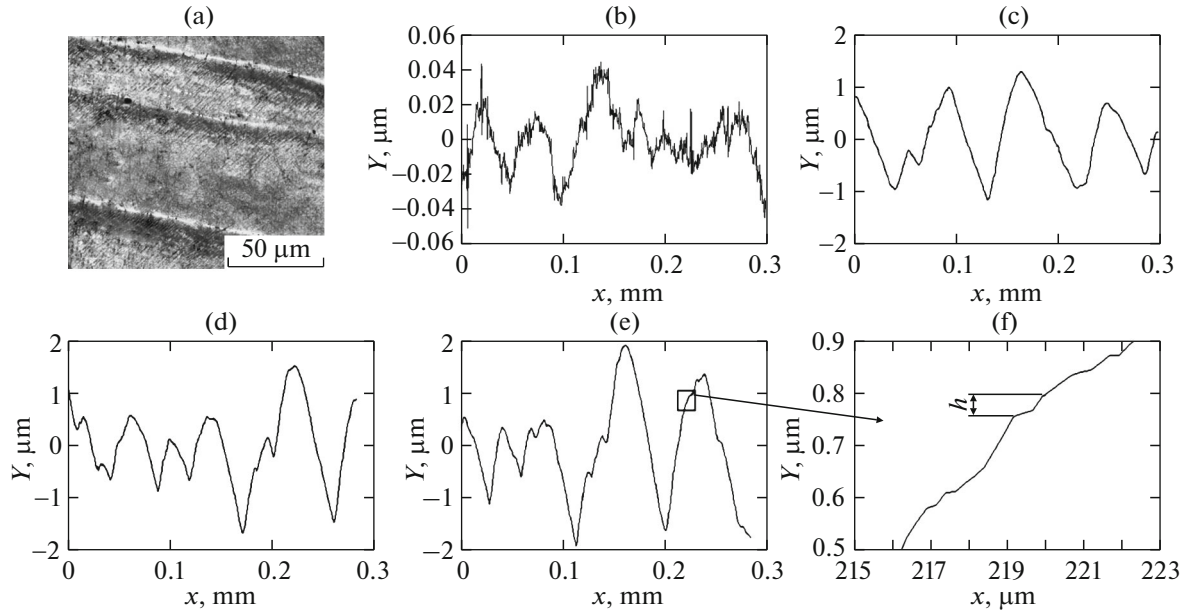

Fig. 1. Evolution of the surface profile in the region of wrinkle formation: (a) deformation relief for ε = 15%; surface profiles for strains of 1.5% (b), 8% (c), 12% (d), and 15% (e); (f) shear steps h (a fragment of the curve in (e)).

height–height function $H(r)$ or, which is the same, as the value corresponding to the first maximum of the autocorrelation function $A(r)$ [29]. Analysis of experimental results has shown that the corrugated (wrinkled) structures under investigation form a mounded surface. The results on the value of λ determined for the case under investigation are given in Table 1.

In addition, autocorrelation function $A(r)$ reflects the relation between the deformations in different local regions and makes it possible to judge about the interaction of local regions separated by different intervals. In fact, correlation radius r_c is the size of the 3D region with self-consistent straining. The correlation radii for corrugated structures are given in Table 1. Analysis of the results indicates that mesovolumes of a size of about 55 μm initially exhibit self-consistent deformation. With increasing strain, we can observe a decrease in the size of the regions of mutual effect to 18–23 μm. Comparison of wavelength λ with correlation radius r_c shows that from 3 to 4 self-consistent deformation zones fit into length λ. Therefore, we observe several levels of self-organization of deformation. A decrease in the matched deformation zone facilitates localization of strain, which is disadvantageous as it regards the preservation of integrity of the strained crystal. It follows hence that the ability of a material to structural self-organization, which would effectively dissipate the loading energy, decreases. Consequently, other deformation mechanisms should be actuated to preserving the integrity of the crystal. Such mechanisms can be stress relaxation due to the rearrangement of the dislocation structure and the evolution of rotational plasticity modes.

Analysis of the behavior of the resultant height–height correlation functions $H(r)$ has made it possible to single out segment L_1 and L_2 on the curve on which the experimental points can be approximated by straight lines with different slopes relative to the axes (Fig. 2). This makes it possible to determine the Hurst exponent and the upper boundaries of the correlation length for several segments (see Table 1). On segment L_3, it is impossible to approximate experimental data with the help of a straight line because of their fluctuation behavior. This indicates the lack of stable correlation on this size scale (Fig. 2a). However, when the strain attains 18%, the third correlation length L_3 can be singled out (Fig. 2b).

Hurst exponent H can be used for analyzing the degree of randomization (self-organization) of the system [30]. A value of the Hurst exponent smaller than 0.5 indicates the antipersistent ergodic type of the system (i.e., the system strives to return to the average

Table 1. Characteristics of a corrugated (wrinkled) deformation relief

Strain ε, %	λ, μm	H_1	H_2	L_1, μm	L_2, μm	r_c, μm
1.5	–	0.002	0.009	2	120	55
8	83	0.017	0.040	3	18	23
12	84	0.018	0.046	2	15	20
15	80	0.022	0.067	1.5	10	22
18	82	0.012	0.049/0.071*	1.2/7*	10	18

*Three scaling levels are singled out on the graph.

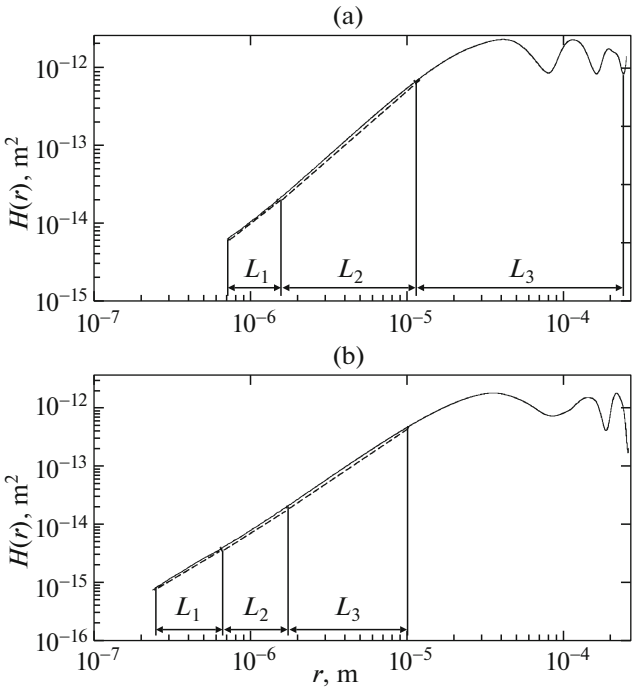

Fig. 2. Height–height correlation function in the region of wrinkle formation on the (112) lateral face of a [111] nickel single crystal: (a) $\varepsilon = 15\%$; (b) $\varepsilon = 18\%$ (dashed curves are approximations of the segments of the solid curves).

value); in this case, the degree of stability of the system depends on the closeness of the value of H to zero. The value of $H = 0.5$ indicates the absence of a correlation. Conversely, the values exceeding 0.5 indicate the existence of long-scale correlations [31].

Analysis of the results shows that for $\varepsilon = 1.5\%$, the deformation is of the antipersistent type (i.e., the system experiences significant changes). On a smaller-scale level, this tendency is manifested more strongly. The case considered here corresponds to the beginning of plastic deformation, when the plastic deformation processes are associated with the evolution of a shear in the bulk of the single crystal and simple material rotations [32]. In all probability, the main sources of dislocations are microscale surface stress concentrators [33], and relaxation is due to counter shears. Owing to such "favorable" conditions, the size of the region with self-consistent deformation amounts to 55 μm. It should be noted that the ability of the system to self-organization at the level of the dislocation subsystem is very high in the entire range of strains under investigation.

With increasing strain, an increase in the Hurst exponent and a decrease in the size of the zone with self-consistent deformation can be observed. As before, sources of dislocations are stress microconcentrators and their stress relaxation occurs via a redistribution of dislocations and the accumulation of the excess dislocation density. The distribution of dislocations exhibits the features of self-organization more clearly [33, 34]. In this case, the formation of a cellular dislocation structure begins. At the third stage, the cellular dislocation substructure continues its evolution, and a transition to a disoriented cellular dislocation structure takes place [26]. At the second and third stages, the cells in fcc materials with high and moderate values of packing defect energy are known to play a significant role in the plastic deformation and hardening. Dislocation cells produce barriers for the motion of dislocations. At the third stage, the cells become disoriented, experience fracture, and subboundaries determining the evolution of the microband substructure appear. In this case, traces with a large shear strain appear. At the microscopic level, the self-consistent motion of dislocations produces plastic deformation of the crystal as before [32]. An insignificant increase in the Hurst exponent in this case indicates that the clearly manifested tendency to the quasi-periodic formation of the profile persists. Apparently, the increasing role of cooperative processes in the dislocation substructure ensures a smaller increase in the Hurst exponent on correlation length L_1 than on correlation length L_2. However, the Hurst exponent on the strain interval under investigation (1.5–18%) does not attain a value of 0.5; i.e., the system remains correlated and tends to self-organization on the scale levels considered here. Otherwise, stress relaxation is not so effective, and this leads to fracture of the crystal. Such cases are described in the literature. In [31], the existence of two zones with the values of the Hurst exponent of 0.3–0.4 and 0.5–0.6 was established for an aluminum alloy after dynamic loading; these zones form the fracture surface. The intervals of determined scales is 1–18 μm. According to the results obtained in [35], the values of the Hurst exponent in the fracture region amount to 0.64–0.81 depending on the experimental conditions. In addition, it is worth considering the fact that the Hurst exponent for many natural phenomena lie in the interval 0.72–0.74 according to the available data [36]. In the description of the deformation relief for different modes of loading, the Hurst exponent also exceeds 0.5 [35, 37–39]. A number of such experiments were performed on measuring segments of a few millimeters, which made it possible to determine the values of the Hurst exponent on the macrolevel and led to the conclusion that self-organization on a large scale is of a type differing from that on the levels described in this study.

It should be noted that when the strain attains a value of 18%, three segments can be singled out of the height–height correlation function. This is due to the actuation of a new mechanism of organization of plastic deformation at the level of the dislocation subsystem, viz., the formation of misoriented microbands, as well as disorientations of a larger scale. Our experiments with nickel single crystals obtained by diffraction of reflected electrons revealed that most clearly

manifested disorientation spreads over a depth of 350–380 μm from the sample surface.

Thus, we can single out the following scale levels of self-organization of plastic deformation of a crystal: the level of the dislocation structure, viz., the microlevel (corresponding to L_1), the level of the group of parallel shear traces, viz., mesolevel (corresponding to L_2), and the mesolevel L_3 associated with the formation of misoriented region. The changes in the type of the dislocation substructure under deformation, the relief parameters, and the values of the Hurst exponent are found to be interrelated.

Since the surface profile in the zone of formation of corrugated structures is alteration of humps and pits, it determines the local curvature of the surface. Each pit is a local zone of a negative curvature of the surface in which additional compressive stresses σ_a appear. Using the relations of mechanics, we can estimate additional compressive stress σ_a by the formula

$$\sigma_a = \sigma_0 w,$$

where σ_0 is the stress in the sample, $w = (1 + 2(a/r)^{-1/2})$, a is the depth of a pit of the profile, and r is the profile radius of curvature. It is coefficient w that in fact shows the degree of elevation of the local stress in the zone of pit formation.

We have calculated coefficient w for various strains. The results together with the values of the Hurst exponent are shown in Fig. 3. Analysis shows that with increasing strain, the additional local stress in the zone of pit formation increases (by about 14% as compared to extreme strains of 8% and 18%). At the same time, the Hurst exponent H_2 also increases, indicating that the tendency to self-organization of the system at the mesolevel is slightly less stable than at the microlevel at which Hurst exponent H_1 practically does not increase and even decreases upon a transition between the third and fourth stages (the tendency to self-organization increases).

In addition, the values of the Hurst exponent H_1 at the microlevel are quite close in the entire range of strains considered here, which indicates the self-similar type of organization of deformation in the entire range of strains. It can be noted that a change in the deformation stage is accompanied with a certain increase in the Hurst exponent H_1 (see Fig. 3), which reflects the evolution in the dislocation structure. Hurst exponent H_2 also increases upon a change in the deformation stages. At the same time, the increase in the Hurst exponent was attributed in [31] to the stage nature of the process of dynamic localization of plastic deformation. An increase in the correlation length upon a change of stages was also noted in [40].

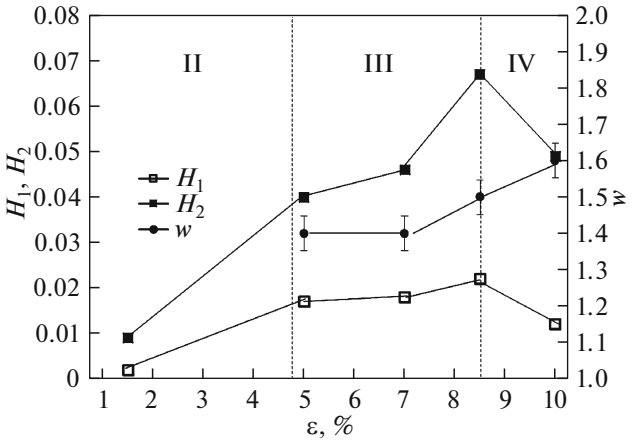

Fig. 3. Dependences of Hurst exponents H_1, H_2 and coefficient w on strain ε (stages II, III, and IV of the deformation curves).

CONCLUSIONS

1. It has been established that corrugated (wrinkled) structures have mounded surfaces with a regular arrangement of mounds with a long-range length scale (wavelength) λ.

2. Using fractal analysis, we have determined the values of the Hurst exponent and correlation lengths for a corrugated (wrinkled) structure. The difference between Hurst exponents H_1 and H_2 indicates that self-organization at the micro- and mesoscale levels is governed by different mechanisms. At the microlevel, it is due to self-organization of the dislocation stricture, while at the mesolevel, due to correlated shear in parallel slip planes.

3. It has been found that upon the attainment of a strain of 18%, the third value L_3 of the correlation length can be established. This can indicate the actuation of an additional mode of self-organization of deformation (misorientation of local regions).

4. We have established the qualitative relation between Hurst exponents H_1, H_2 and coefficient w characterizing the extent of increase in the local stress upon a change of the deformation stage.

ACKNOWLEDGMENTS

The reported study was funded by RFBR, according to the research project no. 16-32-60007 mol_a_dk.

REFERENCES

1. J. P. Hirth and J. Lothe, *Theory of Dislocations* (McGraw-Hill, New York, 1968).
2. V. V. Gubernatorov, T. S. Sycheva, and A. I. Pyatygin, Fiz. Mezomekh. **7** (S2), 97 (2004).
3. V. V. Gubernatorov, B. K. Sokolov, I. V. Gervas'eva, and L. R. Vladimirov, Fiz. Mezomekh. **2** (1–2), 157 (1999).
4. V. V. Gubernatorov, T. S. Sycheva, L. R. Vladimirov, V. S. Matveeva, A. I. Pyatygin, and M. B. Mel'nikov, Fiz. Mezomekh. **5** (6), 95 (2002).

5. B. K. Sokolov, A. K. Sbitnev, V. V. Gubernatorov, I. V. Gervasyeva, and L. R. Vladimirov, Textures Microstruct. **26–27**, 427 (1995).
6. V. V. Gubernatorov, B. K. Sokolov, L. R. Vladimirov, and I. V. Gervasyeva, Textures Microstruct. **32**, 41 (1999).
7. N. K. Sundaram, Y. Guo, and S. Chandrasekar, Phys. Rev. Lett. **109**, 106001 (2012).
8. N. Beckmann, P. A. Romero, D. Linsler, M. Dienwiebel, U. Stolz, M. Moseler, and P. Gumbsch, Phys. Rev. Appl. **2**, 064004 (2014).
9. M. N. Hamdan, A. A. Al-Qaisia, and S. Abdallah, Int. J. Mod. Nonlinear Theory Appl. **1** (3), 55 (2012).
10. S. Khoddam, H. Beladi, P. D. Hodgson, and A. Zarei-Hanzaki, Mater. Des. **60**, 146 (2014).
11. A. Auguste, L. Jin, Z. Suo, and R. C. Hayward, Soft Matter **10**, 6520 (2014).
12. S.-J. Yu, Thin Solid Films **558**, 247 (2014).
13. H. Hirakata, T. Maruyama, A. Yonezu, and K. J. Minoshima, Appl. Phys. **113**, 203503 (2013).
14. J. Y. Chung, J.-H. Lee, K. L. Beers, and C. M. Stafford, Nano Lett. **11**, 3361 (2011).
15. A. Roy, S. Kundu, K. Müller, A. Rosenauer, S. Singh, P. Pant, M. P. Gururajan, P. Kumar, J. Weissmüller, A. K. Singh, and N. Ravishankar, Nano Lett. **14**, 4859 (2014).
16. V. E. Panin and A. V. Panin, Fiz. Mezomekh. **8** (5), 7 (2005).
17. V. P. Alekhin, *The Physics of Surface Strength and Plasticity* (Nauka, Moscow, 1983).
18. V. E. Panin, Fiz. Mezomekh. **2** (6), 5 (1999).
19. V. P. Alekhin, Konstr. Kompoz. Mater., No. 3, 53 (2005).
20. E. A. Alferova and D. V. Lychagin, Appl. Mech. Mater. **379**, 66 (2013).
21. D. V. Lychagin and E. A. Alfyorova, Phys. Solid State **57**, 2034 (2015).
22. D. V. Lychagin, E. A. Alferova, and V. A. Starenchenko, Fiz. Mezomekh. **13** (3), 75 (2010).
23. D. V. Lychagin, S. Y. Tarasov, A. V. Chumaevskii, and E. A. Alfyorova, Appl. Surf. Sci. **371**, 547 (2016).
24. H.-N. Yang, Y.-P. Zhao, A. Chan, T.-M. Lu, and G.-C. Wang, Phys. Rev. B **56**, 4224 (1997).
25. M. Pelliccione and T.-M. Lu, *Evolution of Thin Film Morphology. Modeling and Simulations* (Springer, New York, 2008).
26. S. I. Gubkin, *Flow of Metals* (Metallurgizdat, Moscow, 1961).
27. M. Pelliccione, T. Karabacak, C. Gaire, G. C. Wang, and T. M. Lu, Phys. Rev. B **74**, 125420 (2006).
28. L. Blunt and X. Jiang, *Advanced Techniques for Assessment Surface Topography: Development of a Basis for 3D Surface Texture Standards "SURFSTAND"* (Kogan Page Science, London, 2003).
29. O. Wouters, W. P. Vellinga, R. van Tijum, and J. T. M. De Hosson, Acta Mater. **54**, 2813 (2006).
30. V. N. Aptukov, V. Yu. Mitin, and A. P. Skachkov, Vestn. Permsk. Univ. Mat. Mekh. Inf. **4** (4), 30 (2010).
31. E. A. Lyapunova, A. N. Petrova, I. G. Brodova, O. B. Naimark, M. A. Sokovikov, V. V. Chudinov, and S. V. Uvarov, Fiz. Mezomekh. **15** (2), 61 (2012).
32. V. E. Panin and L. E. Panin, Fiz. Mezomekh. **7** (4), 5 (2004).
33. N. A. Koneva, Soros. Obraz. Zh., No. 6, 99 (1996).
34. G. A. Malygin, Phys.-Usp. **42**, 887 (1999).
35. V. A. Oborin, M. V. Bannikov, and O. B. Naimark, Vestn. Permsk. Nats. Issled. Politekh. Univ. Mekh., No. 2, 87 (2010).
36. J. Feder, *Fractals* (Plenum, New York, 1988).
37. V. Oborin, M. Bannikov, O. Naimark, and C. Froustey, Tech. Phys. Lett. **37**, 241 (2011).
38. V. A. Oborin, O. B. Naimark, U. Ran, and A. Koroleva, Vestn. Permsk. Univ. Fiz. **4** (22), 4 (2012).
39. M. Zaiser, F. M. Grasset, V. Koutsos, and E. C. Aifantis, Phys. Rev. Lett. **93**, 195507 (2004).
40. P. V. Kuznetsov, V. E. Panin, K. V. Levin, A. G. Lipnitskii, and J. Schreiber, Fiz. Mezomekh. **3** (4), 89 (2000).

Translated by N. Wadhwa